

Abdominal Organ Segmentation Using Patch-based 3D UNet with Attention

Xue Feng¹

¹Biomedical Engineering, University of Virginia

xf4j@virginia.edu

Abstract. In this application, we have developed a 3D UNet method with attention blocks for abdominal organ segmentation. To address the variability in the field-of-view, we applied a pre-processing to crop the images to only contain the abdominal regions. In training the network, a random patch selection with high bias towards the positive labels (90%) was used. A weighted sum of Dice and cross entropy loss was used during training. In post-processing, we removed non-connected regions that are smaller than a given ratio of the maximum region as the organs are clustered.

Keywords: 3D U-Net, Attention Block, Abdominal Organ Segmentation

1. Introduction

Abdominal organ segmentation is a challenging task due to the varied contrast, coverage, and disease conditions. In this study we've developed a 3D UNet method for automatic organ segmentation for liver, spleen, kidney, and pancreas. Attention blocks were used to let the network focus more on the target region-of-interest.

2. Method

Figure 1 illustrates the applied 3D U-Net, where a U-Net [1] architecture is adopted.

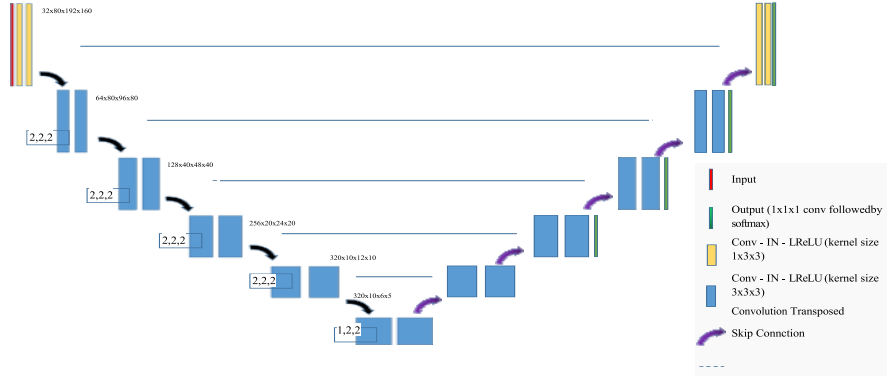


Figure 1. Network architecture

2.1. Preprocessing

- Cropping strategy: to handle the variability in the coverage along the superior-inferior direction, we set a maximum field-of-view (FOV) of 500 mm along this direction; for the cases that exceed this limit, we first detected the lung slice and chosen the slice that contains the most lung voxels as the top most slice and crop the rest from the inferior direction.
- Resampling method for anisotropic data: the image is resampled to a uniform voxel spacing of 1mm * 1mm * 3 mm (out-of-plane) using linear interpolation.

- Intensity normalization method: the intensity is cropped to -1000 to 600 in HU values and then normalized to be zero mean and unit variance.

2.2. Proposed Method

- Network architecture details: we used a 3D U-Net model with attention blocks.
- Loss function: we use the summation between Dice loss and cross entropy loss because it has been proved to be robust [3] in various medical image segmentation tasks. In addition, the loss for each organ is weighted differently. In this case, liver weights is set to be 1, weights for all other organs are set to be 4.

2.3. Post-processing

A connected component analysis of all ground truth labels is applied. For each organ, remove the non-connected regions that have the area smaller than a ratio of the maximum area. For liver, spleen, and pancreas, the ratio is set to be 1; for kidney, the ratio is set to be 1/3.

3. Dataset and Evaluation Metrics

3.1. Dataset

- A short description of the dataset used:
The dataset used of FLARE2021 is adapted from MSD [4] (Liver [5], Spleen, Pancreas), NIH Pancreas [6, 7, 8], KiTS [9, 10], and Nanjing University under the license permission. For more detail information of the dataset, please refer to the challenge website and [11].
- Details of training / validation / testing splits:
The total number of cases is 511. Due to the limited time, we trained a final model using all 511 cases and did not perform any validation studies.

4. Implementation Details

4.1. Environments and requirements

The environments and requirements of the baseline method is shown in Table 2.

Table 2. Environments and requirements.

Windows/Ubuntu version	Ubuntu 18.04.5 LTS
CPU	Intel(R) Xeon(R) CPU E5-2603 v4 @ 1.70GHz
RAM	16×4GB
GPU	Nvidia 2080 Ti
CUDA version	11
Programming language	Python3.6
Deep learning framework	Tensorflow 2.3
Specification of dependencies	SimpleITK
(Optional) code is publicly available at	

4.2. Training protocols

The training protocols of the baseline method is shown in Table 3.

Table 3. Training protocols.

Data augmentation methods	Rotations, scaling, Gaussian noise, Gaussian blur, brightness, contrast, simulation of low resolution, gamma correction and mirroring.
Initialization of the network	“he” normal initialization

Patch sampling strategy	90% of the samples in a batch contain at least one randomly chosen foreground class.
Batch size	1
Patch size	64 * 192 * 192
Total epochs	2000
Optimizer	Stochastic gradient descent with nesterov momentum ($\mu = 0.99$)
Initial learning rate	0.01
Learning rate decay schedule	poly learning rate policy: $(1 - \text{epoch}/1000)^{0.9}$
Stopping criteria, and optimal model selection criteria	Stopping criterion is reaching the maximum number of epoch (1000).
Training time	96 hours
CO ₂ eq ¹	

4.3. Testing protocols

- Pre-processing steps of the network inputs: The same strategy is applied as training steps.
- Post-processing steps of the network outputs: For each organ, remove the non-connected regions that have the area smaller than a ratio of the maximum area. For liver, spleen, and pancreas, the ratio is set to be 1; for kidney, the ratio is set to be 1/3.
- If using patch-based strategy, describing the patch aggregation method:
The same patch-based strategy is applied as nnU-Net [2]. Voxels close to the center are weighted higher than those close to the border, when aggregating predictions across patches.

5. Results

5.1. Qualitative results

6. Discussion and Conclusion

The baseline method can work well on cases where no diseases exist. Besides, the DSC and NSD scores of liver segmentation is higher than the other organs, indicating liver maybe a comparable easier task as a result of its bigger size and consistent shape. Disappointing performance is obtained for pancreas segmentation as a result of the inter-patient anatomical variability of volume and shape.

The existence of lesion is a critical factor for the segmentation performance. How to properly segment those cases is important. Besides, obtaining an accurate boundary segmentation need further investigate. Moreover, disappointing performance is obtained for pancreas segmentation as a result of the inter-patient anatomical variability of volume and shape.

Acknowledgment

The authors of this paper declare that the segmentation method they implemented for participation in the FLARE challenge has not used any pre-trained models nor additional datasets other than those provided by the organizers.

References

- [1] O. Ronneberger, P. Fischer, and T. Brox, "U-net: Convolutional networks for biomedical image segmentation, in *International Conference on Medical image computing and computer-assisted intervention*, 2015, pp. 234–241. [1](#)
- [2] F. Isensee, P. F. Jaeger, S. A. Kohl, J. Petersen, and K. H. Maier-Hein, "nnu-net: a self-configuring method for deep learning-based biomedical image segmentation," *Nature Methods*, vol. 18, no. 2, pp. 203–211, 2021. [1](#), [2](#), [3](#)
- [3] J. Ma, J. Chen, M. Ng, R. Huang, Y. Li, C. Li, X. Yang, and A. L. Martel, "Loss odyssey in medical image segmentation," *Medical Image Analysis*, vol. 71, p. 102035, 2021. [1](#)
- [4] A. L. Simpson, M. Antonelli, S. Bakas, M. Bilello, K. Farahani, B. Van Ginneken, A. Kopp-Schneider, B. A. Landman, G. Litjens, B. Menze *et al.*, "A large annotated medical image dataset for the development and evaluation of segmentation algorithms," *arXiv*

preprint *arXiv:1902.09063*, 2019. 2

- [5] P. Bilic, P. F. Christ, E. Vorontsov, G. Chlebus, H. Chen, Q. Dou, C.-W. Fu, X. Han, P.-A. Heng, J. Hesser *et al.*, “The liver tumor segmentation benchmark (lits),” *arXiv preprint arXiv:1901.04056*, 2019. 2
- [6] H. Roth, A. Farag, E. Turkbey, L. Lu, J. Liu, and R. Summers, “Data from pancreas-ct. the cancer imaging archive (2016).” 2
- [7] H. R. Roth, L. Lu, A. Farag, H.-C. Shin, J. Liu, E. B. Turkbey, and R. M. Summers, “Deeporgan: Multi-level deep convolutional networks for automated pancreas segmentation,” in *International conference on medical image computing and computer-assisted intervention*. Springer, 2015, pp. 556–564. 2
- [8] K. Clark, B. Vendt, K. Smith, J. Freymann, J. Kirby, P. Koppel, S. Moore, S. Phillips, D. Maffitt, M. Pringle *et al.*, “The cancer imaging archive (tcia): maintaining and operating a public information repository,” *Journal of digital imaging*, vol. 26, no. 6, pp. 1045–1057, 2013. 2
- [9] N. Heller, F. Isensee, K. H. Maier-Hein, X. Hou, C. Xie, F. Li, Y. Nan, G. Mu, Z. Lin, M. Han *et al.*, “The state of the art in kidney and kidney tumor segmentation in contrast-enhanced ct imaging: Results of the kits19 challenge,” *Medical Image Analysis*, vol. 67, p. 101821, 2021. 2
- [10] N. Heller, S. McSweeney, M. T. Peterson, S. Peterson, J. Rickman, B. Stai, R. Tejpaul, M. Oestreich, P. Blake, J. Rosenberg *et al.*, “An international challenge to use artificial intelligence to define the state-of-the-art in kidney and kidney tumor segmentation in ct imaging.” *American Society of Clinical Oncology*, vol. 38, no. 6, pp. 626–626, 2020. 2
- [11] J. Ma, Y. Zhang, S. Gu, C. Zhu, C. Ge, Y. Zhang, X. An, C. Wang, Q. Wang, X. Liu, S. Cao, Q. Zhang, S. Liu, Y. Wang, Y. Li, J. He, and X. Yang, “Abdomenct-1k: Is abdominal organ segmentation a solved problem?” *IEEE Transactions on Pattern Analysis and Machine Intelligence*, 2021. 2, 3, 4